Theor Chem Acc (2001) 106:55–61
DOI 10.1007/s002140000237

Theoretical
Chemistry Accounts

Regular article

Assessment of conformation and energetics of the N-terminal part of elafin via computer simulations

Roman G. Efremov[1], Pavel E. Volynsky[1], Manuel A. M. Dauchez[2], Dmitry E. Nolde[1], Alexander S. Arseniev[1], Alain J. P. Alix[2]

[1] M.M. Shemyakin and Yu.A. Ovchinnikov Institute of Bioorganic Chemistry, Russian Academy of Sciences, Ul. Miklukho-Maklaya, 16/10, Moscow V-437, 117871 GSP, Russia, e-mail: efremov@nmr.ru
[2] Laboratoire de Spectroscopies et Structures Biomoléculaires, Faculté des Sciences, Université de Reims Champagne-Ardenne, IFR53 Biomolécules, B.P. 1039, 51687 Reims Cédex 2, France, e-mail: alain.alix@univ-reims.fr

Received: 5 July 2000 / Accepted: 4 October 2000 / Published online: 28 February 2001

Abstract. Elafin, a specific inhibitor of elastase, is thought to play a regulatory role in inflammation. An NMR-derived solution structure of recombinant elafin has been reported [Francart et al. (1997) *J Mol Biol* 268:666], although the conformation of its flexible N-terminal part is not established. There is experimental evidence that the N terminus (residues 1–15) of elafin interacts with the cell membrane. To explore the conformational preferences of residues in this region, we have performed Monte Carlo simulations of the peptide in water, in cyclohexane, and in a model membrane. Additionally, 3.7-ns molecular dynamics with explicit water was carried out. The main results were that the hydrophobic environment stabilizes an α helix in the region 6–11, the peptide is unordered in water, and it is attached to the membrane via the amphiphilic α-helix 6–11, which inserts with its N terminus forming an angle of about 60° to the membrane plane. We therefore assume that in nonpolar media the N-terminal part of elafin forms a short α helix which might act as a membrane anchor.

Key words: Peptide-membrane interactions – Secondary structure – Protein conformation – Solvation potential – Molecular modeling

1 Introduction

Elafin is a small, 57-residue protein believed to be important in the regulation of elastase-mediated tissue damage [1]. It was simultaneously described in psoriatic skin and bronchial secretions [1, 2] but is present in many tissues [3]. Elafin was shown to be a specific inhibitor of human leukocyte and neutrophil elastases, porcine pancreatic elastase (PPE), and of proteinase-3. Along with several other proteins, elafin comprises an integral part of the ''anti-elastase shield'' in the lung.

The 3D solution structure of recombinant elafin (r-elafin) has been determined by NMR spectroscopy [4]. The structure is characterized by a flat core and a flexible N-terminal part. The former comprises a central twisted β hairpin accompanied by two external segments linked by the proteinase binding loop. Three disulfide bridges connect the external segments to the central β sheet, and a single fourth disulfide bridge links the binding loop to the central β turn. Detailed analysis of the solution structure of r-elafin, along with the X-ray crystallographic structure of elafin complexed with PPE [5], provided considerable insight into the inhibitory mechanism and permitted identification of corresponding structural determinants.

On the other hand, there is experimental support for some other biological activities of elafin. Thus, it plays a role in the regulation of the elastase-driven proteolysis of the extracellular matrix as well as possessing an antimicrobial function [6]. It is involved in the formation of the cornfield cell envelope – a 15-nm thick insoluble layer deposited on the intracellular side of the membrane [7]. In the literature there are indications that in the process of functioning, elafin might be anchored to the cell membrane [6, 7]. Finding which parts of the protein participate in the membrane binding will shed light on its mechanism of action, which is still unclear.

Often, globular proteins interact with a lipid bilayer by means of segments, which can change their structure depending on the environment, for example, rather unordered in aqueous solution and more structured on the water–membrane interface. The elafin molecule is very rigid. It is cross-linked with four disulfide bridges and has no flexible loops, the maximum number of residues between neighboring cysteines being eight. The only

Correspondence to: A. J. P. Alix and/or R. G. Efremov
Contribution to the Symposium Proceedings of Computational Biophysics 2000

exception is the N terminus. This has no defined spatial structure either in the crystal structure of the elafin–PPE complex or in the solution models of r-elafin. Taking this into account, one might propose that this flexible part of the protein part has the capacity to undergo environment-dependent conformational changes and, therefore, to anchor onto the membrane surface. Our previous circular dichroism measurements revealed augmentation of α-helical content of r-elafin upon increasing the hydrophobicity of the environment [8]: the higher the concentration of sodium dodecyl sulfate in solution, the higher the α-helical content of r-elafin. Our assumption is that the observed solvent-induced α-helix formation and the anchoring of elafin on the membrane are associated with its N terminus. It is well established now that the environment, especially the membrane interior or the membrane–water interface, can serve to stabilize an α-helical conformation in proteins and peptides [9, 10].

To check this hypothesis, in the present study we assess solvent-dependent conformational preferences of residues in the N-terminal part 1–15 of elafin ($N_{1–15}$–EL), together with their ability to interact with a membrane. This is done via exhaustive Monte Carlo (MC) and molecular dynamics (MD) simulations of $N_{1–15}$–EL in media of different polarity, including our original implicit solvation model, which mimics a heterogeneous membrane. Taken together, the results show that the N-terminal part of elafin might bind to the cell membrane via the formation of a short interfacial α helix.

2 Materials and methods

2.1 Peptide

In all the simulations we used the peptide $N_{1–15}$–EL with a sequence: AQEPVKGPVSTKPGS. Its starting structures were built both in α-helical (α-helical start) and random-coil (random start) conformations. The peptide was capped and the charges were assigned at pH 7. In calculations with the heterogeneous membrane model, the peptide was taken as an entire α helix disposed outside the hydrophobic layer. To change, during the MC simulation, the orientation of the peptide with respect to the bilayer, a fragment of 11 dummy residues was attached to the N-terminal part. These "virtual" residues did not contribute to the energy of the system. The first atom of the N-terminal dummy residue was always placed in the center of the bilayer with coordinates (0, 0, 0).

2.2 MC simulations

The principal objective of the simulations was to assess the most energetically stable states of $N_{1–15}$–EL in media of different polarity. The conformational space of the peptide was explored in an unrestrained MC search in torsion angle space using the modified FANTOM program [11] and our implicit solvation models for polar (water) and nonpolar (cyclohexane) solvents [12, 13], as well as for a membrane-mimetic heterogeneous environment [14, 15]. The full-atom potential-energy function was taken in the form: $E_{\text{total}} = E_{\text{ECEPP/2}} + E_{\text{solv.}}$, where the term $E_{\text{ECEPP/2}}$ includes van der Waals, torsion, electrostatic and hydrogen-bonding contributions [16]. $E_{\text{solv.}}$ is the solvation energy: $\Delta E_{\text{solv.}} = \sum_{i=1} \Delta\sigma_i \text{ASA}_i$, where $\Delta\sigma_i$ and ASA_i are, respectively, the atomic solvation parameter and the solvent-accessible surface area (ASA) for atom *i*. To cross the energy barriers between local minima, an adaptive-temperature schedule protocol [11] was employed. On each MC step the structures were subjected to conjugate-gradients minimization (Table 1). The ω dihedral angles were fixed (except those in dummy residues), and a spherical cutoff of 30 Å for nonbond interactions was employed. Long-range electrostatic interactions were damped by using distance-dependent dielectric permeability, $\varepsilon = 4r$.

Before the simulations, starting structures were subjected to 500–1000 steps of unconstrained conjugate-gradients minimization. In each media, several consequent MC runs were carried out. In the first stages of the MC protocol, large structural changes were allowed by sampling several dihedrals. Then the fine-tuning conformational search with only a few varied dihedrals was performed (Table 1). The starting structure for each MC run was the lowest-energy one obtained in the previous run.

The set of resulting structures was analyzed using the following parameters: total energy, secondary structure, degree of helicity (N_α – number of residues in an α helix), ASA, angles, θ, of helical segments with the normal to the membrane plane (*z*-axis), hydrogen bonding. The half-width of the interface region and the membrane thickness were taken to be 1.5 and 30 Å, respectively. Analysis of MC data was done using auxiliary programs specially written for this. Along with other details of the computational protocol they are described elsewhere [14, 15].

2.3 Molecular dynamics of $N_{1–15}$–EL in explicit water

The MD for 3.7 ns was calculated using the GROMACS program and force field [17] for the peptide placed in a rectangular box of 2244 single-point charge water molecules with periodic boundary conditions. The starting structure of $N_{1–15}$–EL represented an ideal capped α helix. Initially, the peptide was fixed, and solvent molecules were relaxed using 5000 iterations of steepest descent energy minimization. Then the peptide and water system was subjected to a 5-ps MD run with fixed atoms of $N_{1–15}$–EL. Finally, the system was heated from 5 to 300 K over 20 ps followed by 3.7 ns of an unrestrained MD collection run at 300 K. Long-range electrostatic interactions were truncated with a cutoff of 9 Å using the particle-mesh Ewald sum method [17]. van der Waals interactions were truncated using a shifting function with characteristic parameters 7 and 9 Å. Analysis of the MD trajectory was carried out using the GROMACS software.

The secondary structure, the ASA, and the hydrogen bonding were analyzed using the DSSP program [18]. Ribbon diagrams of the

Table 1. Computational protocols used in Monte Carlo (*MC*) simulations of $N_{1–15}$–EL in different environments. Each run includes 500 MC steps; $N_{\text{dih.}}$ and $N_{\text{minim.}}$ are the numbers of randomly chosen dihedrals and unconstrained conjugate-gradient minimizations on each MC step

Environment	Starting conformation					
	α helix			Random coil		
	MC run	$N_{\text{dih.}}$	$N_{\text{minim.}}$	MC run	$N_{\text{dih.}}$	$N_{\text{minim.}}$
Water	1	3	70	1	10	60
	2	3	70	2	5	60
	3	1	70	3	2	60
				4	1	60
Cyclohexane	1	5	60	1	5	60
	2	3	60	2	3	60
	3	3	60	3	3	60
	4	2	60	4	2	60
	5	1	60	5	1	60
	6	1	100	6	1	70
				7	1	100
Membrane	1	5	70			
	2	2	70			
	3	2	70			
	4	1	70			
	5	1	100			
	6	1	80			

molecules were produced with the MOLMOL program [19]. The molecular hydrophobicity potential (MHP) created by peptide atoms in the surface points of the helical segment 6–11 (with added N-acetyl and N-methyl groups on the termini) was calculated and visualized by means of 2D isopotential plots in coordinates (α,z), where α is the rotation angle around the helix axis and z coincides with the helix axis. This was done as described earlier [20, 21]. The α-helical structures used for the MHP calculations corresponded to the lowest-energy states found in the results of the MC simulations in membrane-mimetic media. The helix-forming propensities of residues in N_{1-15}–EL were calculated on the basis of its sequence, in the framework of the modified Lifson–Roig helix–coil model [22, 23].

3 Results and discussion

3.1 N_{1-15}–EL in water

3.1.1 MC conformational search

Results of MC simulations obtained with both α-helix and random starts, were analyzed as one set of data. In total, 1862 different conformational states were accumulated. Depending on their secondary structure and pairwise root-mean-square deviations, they were further subdivided into different groups. The energy levels and conformations of the three groups of the most stable states are shown in Fig. 1. We should point out that each state shown in Fig. 1 represents a local minimum on the potential-energy hypersurface of the peptide and water system. It is seen that regardless of the starting structure, the lowest-energy states (states 1 and 2 in Fig. 1) are unordered. They are separated from the closest states containing a short fragment of the α helix (residues Pro8-Thr11, state 3 in Fig. 1) by an energy gap of about 11 kcal/mol. The most energetically favorable structures are stabilized by several intramolecular hydrogen bonds and contain β-reverse turns (e.g., Glu-Pro-Val-Lys and Lys-Pro-Gly-Ser in the lowest-energy conformer).

Simulations with surface-based implicit solvent models similar to that employed here were successfully applied to a number of proteins and peptides [24]. On the other hand, we should point out that such an approximation does not take into account protein–water hydrogen bonding, which plays an important role in helix stabilization/destabilization by water molecules. Therefore, to check our findings on the N_{1-15}–EL behavior in polar media, we performed a MD simulation in an explicit water environment. The starting structure was taken as the entire α helix.

3.1.2 Molecular dynamics of N_{1-15}–EL in explicit water

The locations of the secondary structure elements, the total ASA, and the numbers of intramolecular and intermolecular hydrogen bonds of the peptide are displayed versus time in Fig. 2. An unfolding event during the simulation is shown in Fig. 3. Analysis of the MD trajectory permits the following conclusions to be drawn.

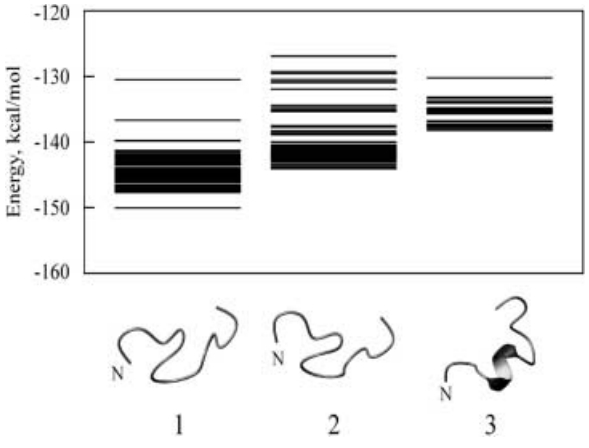

Fig. 1. (*Top*) Low-energy conformers of N_{1-15}–EL obtained as the result of a Monte Carlo conformational search with an implicit water model. Levels of the total energy for different classes of conformers. The conformers are grouped according to their pairwise root-mean-square deviations (*rmsd*) and secondary structure. Inside the same group, all the conformers have identical secondary structure and maximal pairwise rmsd 1 Å (taken over C_α atoms). (*Bottom*) Ribbon diagrams of the conformers of groups 1–3 (calculated for the minimal-energy structure from the corresponding group)

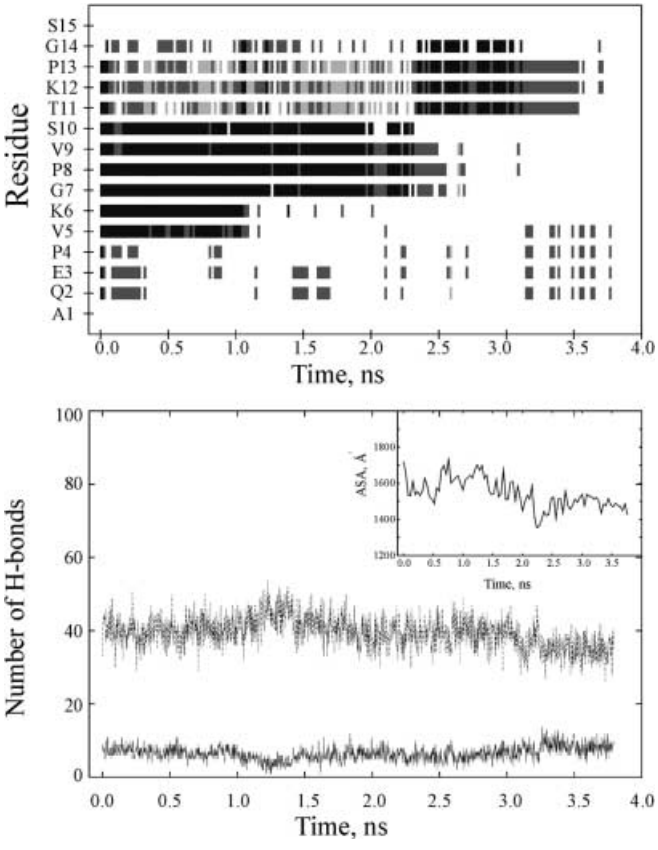

Fig. 2. (*Top*) The locations of the secondary structure elements (every 20 ps) during molecular dynamics simulation of N_{1-15}–EL in explicit water. *Black*, *dark-gray*, *medium-gray*, and *light-gray* bars show the location of α helix, 3_{10} helix, β turns and bends, respectively (abbreviated as H, G, T, S by the DSSP program [18]). (*Bottom*) Total accessible surface area (*ASA*) (*insert*) and numbers of intramolecular (*bottom curve*) and intermolecular hydrogen bonds of the peptide versus time

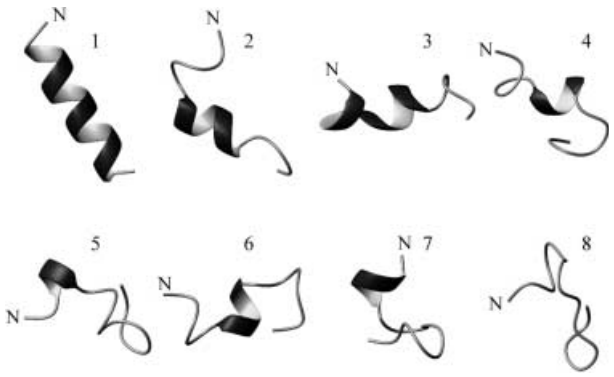

Fig. 3. Snapshots of the conformations of $N_{1–15}$–EL illustrating an unfolding event during molecular dynamics simulation in explicit water. The conformations at 0, 0.282, 1.040, 1.654, 2.02, 2.110, 3.02, and 3.670 ns are indicated by numbers 1–8, respectively. Side chains of residues are not shown. The N terminus of the peptide is marked by the letter *N*

1. The α helix undergoes rapid (10–40 ps) destabilization on residues Gln2, Glu3, Pro4, Thr11, Lys12, Pro13, and Gly14 (Fig. 2, up).
2. In the time interval 0.1–2.2 ns, the region Thr11-Pro13 reveals a bifurcating 3_{10} helix, which then transforms into the α helix 11–14 and lives until 3.2 ns.
3. The most stable α helix is observed in the region 7–10: it exists during the first 2.3 ns of the dynamics.
4. A number of β turns are detected: most frequently they occur near the peptide termini (residues 1–5 and 11–14). Interestingly, during the MD run, β turns on the C terminus consequently compete with the 3_{10} helix ($t < 2.3$ ns) and the α helix ($t > 2.3$ ns).
5. Inspection of the values of the ASA of $N_{1–15}$–EL, as well as intramolecular and intermolecular hydrogen bonds, shows that unfolding of the peptide is not accompanied by an increase in the ASA (Fig. 2, insert). During all the simulation, the number of protein–water hydrogen bonds also stays quite stable. That is also true for intrapeptide hydrogen bonds, although their nature is different at the beginning and at the end of the dynamics run: in the former there are many hydrogen bonds of type $i \rightarrow i + 4$, while in the latter only bonds of the types $i \rightarrow i + 1$ and $i \rightarrow i + 2$ are observed. Destabilization of the helical structure progressively occurs on the N terminus, while its central and (partly) C-terminal parts preserve the folded state until 2.5 and 3.2 ns, respectively.

The results obtained through MC and MD simulations in implicit and explicit aqueous solution agree fairly well with each other. Thus, the N-terminal part of elafin appears to be flexible and unordered in water – the lowest-energy states found by the MC technique and the structures observed during last 500 ps (3.2–3.7 ns) of dynamics, have no residues in the α-helix or the 3_{10}-helix conformation. This is consistent with X-ray [5] and NMR [4] data, where the 3D structure was not resolved. In both computational experiments the highest α-helix propensities were found for residues 7–10 disposed in the middle part of $N_{1–15}$–EL. In contrast, β turns are preferentially distributed near the peptide termini.

3.2 $N_{1–15}$–EL in homogeneous nonpolar media (cyclohexane)

Analysis of the conformations of $N_{1–15}$–EL accumulated as the result of the MC search in nonpolar media (cyclohexane) implies that a hydrophobic environment considerably stabilizes the central part of the peptide (residues 6–11 Lys-Gly-Pro-Val-Ser-Thr and/or 7–11 Gly-Pro-Val-Ser-Thr) in an α-helical conformation. Corresponding states have energies of about 12 kcal/mol (from −118 to −106 kcal/mol) and are separated from the nearest nonhelical ones by an energy gap which exceeds 10 kcal/mol (Fig. 4). In addition to hydrogen bonds of the type $i \rightarrow i + 4$ inherent in the α helix, the lowest-energy structures reveal β turns near the N terminus (residues Glu-Pro-Val-Lys). For the low-energy conformers the numbers of backbone–backbone hydrogen bonds are systematically higher than those in water. Interestingly, the helical region includes Gly-7 and Pro-8 residues, which are known as "helix breakers" in globular proteins and in aqueous solution [25]. This confirms previous experimental [9] and theoretical [13, 26] results on the stabilization of an α helix at the membrane–water interface. We should note that highest helix propensities for residues 6–11 of $N_{1–15}$–EL in nonpolar media correlate well with those observed via MD simulation in explicit water (see earlier). At the same time, the total balance of intramolecular and intermolecular interactions for α helix 6–11 is favorable in cyclohexane and is unfavorable in water.

3.3 $N_{1–15}$–EL in the heterogeneous model membrane

Although simulations with the ASP models mimicking bulk media of different polarity permit evaluation of

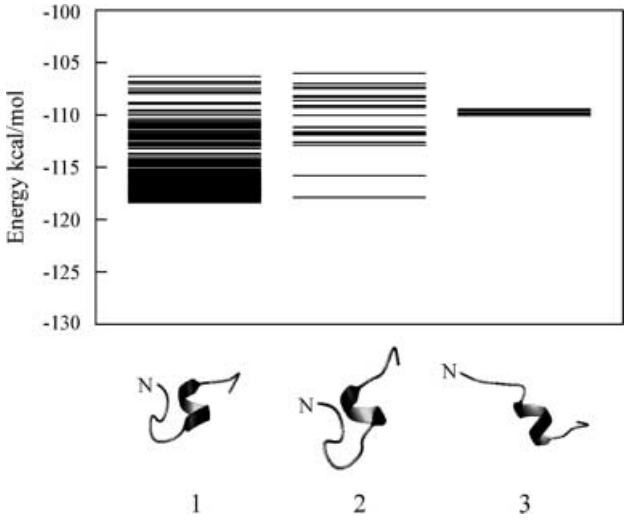

Fig. 4. Low-energy conformers of $N_{1–15}$–EL obtained as the result of the Monte Carlo conformational search in nonpolar media (cyclohexane). All the details are as in the legend to Fig. 1

principal trends in the solvent-induced structural behavior of N_{1-15}–EL, a hypothesis about its possible interaction with a cell membrane demands that the heterogeneous nature of the water–bilayer interface be taken into account. Several important questions arise:

1. Whether the peptide prefers to be solvated by water molecules, stays adsorbed on the membrane surface, or inserts into its hydrophobic zone.
2. If membrane binding occurs, what residues are involved?
3. What are the conformational states of the membrane-bound peptide?
4. What might be the energetic cost of peptide insertion?

To address these questions, we performed an unrestrained MC conformational search for N_{1-15}–EL in a recently developed heterogeneous membrane-mimetic environment [14, 15].

Using this technique, 2353 different conformational states (local minima) were obtained. Their analysis implies that, as in pure apolar media, fragment 6–11 has a prominent tendency to form an α helix which lies on the interface and inserts itself into the hydrophobic zone by about 1.5 Å with its N terminus (Fig. 5). The angle between the helix axis and the membrane plane is about 60°. These states are stable over a wide range of energies: −155, −140 kcal/mol. Residues Pro-4, Val-5, Lys-6, and Val-9 are sufficiently buried into the membrane, whereas the others are exposed to the polar phase. Another group (group 2) of the low-energy states shown in Fig. 5 reveals an α helix only in the region 8–11. The most stable conformer of this set is 5.4 kcal/mol higher in energy compared with those in group 1. All residues in these structures (except Val-5) are located outside the hydrophobic zone, which corresponds to the lipid acyl chain region of the membrane. Somewhat higher energies are observed for the third group of states. They are characterized by 3_{10}-helical (residues 4–6) and α-helical (residues 7–11) regions. The N terminus of such a "combined" helix is buried about 1.2 Å into the hydrophobic core. Residues Pro-4, Val-5, Pro-8, Val-9 strongly interact with the membrane. As with the cyclohexane analysis, the low-energy states are characterized by significant numbers of intramolecular hydrogen bonds between the backbone atoms (normally they have 6–7 such bonds).

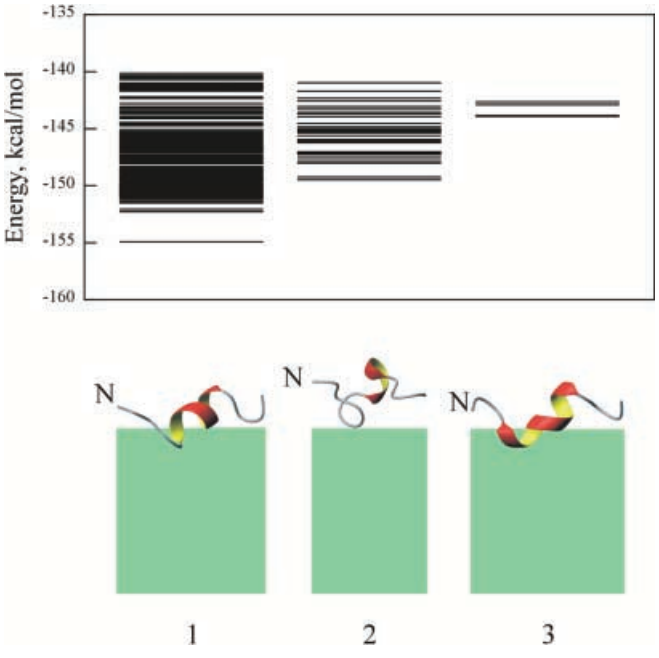

Fig. 5. Low-energy conformers of N_{1-15}–EL obtained as the result of the Monte Carlo conformational search with the implicit membrane model. The membrane is shown with a *gray* hatching. Other details are as in the legend to Fig. 1

To assess the factors determining the stability of the membrane-bound helix 6–11 (group 1, Fig. 5), we calculated all the energy components of this state in three different media – in a membrane, water, and cyclohexane. The corresponding values of the total energies are −150.49, −144.38, and −109.78 kcal/mol. These differences are caused only by the solvation terms ($E_{solv.}$) – the contributions of intramolecular interactions are equivalent because of the identity of the conformations. Therefore, in a membrane $E_{solv.}$ is about 6 and about 41 kcal/mol lower than in water and nonpolar solvent, respectively. We should note that the observed stability of the membrane-bound state of N_{1-15}–EL is not a trivial fact. Analysis of the sequence of N_{1-15}–EL using standard hydropathy techniques [27] suggests that the peptide is heavily polar (with an average hydrophobicity index, $\langle H \rangle$, of −0.060). Moreover, calculations with a seven-residue sliding window show that it does not contain even short hydrophobic segments with $\langle H \rangle > 0.180$. Among these segments, the membrane-bound one predicted here (6–11), is the most hydrophilic with $\langle H \rangle = -0.221$ and a low value for the hydrophobic moment. Another approach, which is often used to assess helix-forming propensities of residues in peptides, is based on the modified Lifson–Roig theory of the helix–coil transition [22]. In this approximation, the highest probabilities of the α-helical conformation (both in water and in 40% trifluoroethanol) are assigned to residues Gln-2, Glu-3, Val-9, Ser-10, Thr-11, and Lys-12, while the lowest ones are assigned to residues Pro-4, Gly-7, Pro-8, Pro-13, and Gly-14. Evidently, these results drastically differ from those obtained here via MD and MC simulations. A conclusion could be made that the analysis based solely on the sequence information fails to delineate putative sites of interaction with a membrane. It is therefore necessary to inspect the hydrophobic properties of the α-helical region 6–11 in more detail.

To investigate this, we calculated the MHP on its surface. The formalism of MHP utilizes a set of atomic physicochemical parameters evaluated from octanol–water partition coefficients (log *P*) of numerous chemical compounds [28]. The MHP approach takes into the consideration of the heterogeneous nature of the peptide's side chains, their conformation, and the microenvironment in the 3D structure [21] and, therefore, permits detailed assessment of the hydrophobic and/or hydrophilic properties of various parts of the molecules (e.g., it provides a pictorial 2D representation of non-

polar and polar patterns on the surfaces of the helix). Previously, we developed an MHP-based molecular modeling approach to analyze the spatial polarity properties of membrane-bound peptides and to assess their mode of interaction between each other and with the membrane [20].

3.4 Hydrophobic properties of the α helix 6–11 – a potential membrane anchor

The 2D isopotential contour map MHP(α, *z*) for α helix 6–11 of $N_{1–15}$–EL is displayed in Fig. 6. The map is a projection of the MHP values calculated in the surface points of the peptide onto a cylinder with a *z*-axis corresponding to the helix axis. α is the rotation angle around the helix axis. The function MHP(α, *z*) was obtained for the lowest-energy conformer of group 1 (Fig. 5) found in the MC simulations. It is seen that on the helix surface there is a tilted polarity pattern formed by residues Gly-7 and Ser-10 as well as by polar side chains of Lys-6 and Thr-11. The broken line in Fig. 6 labels the position of the membrane interface: the part of the surface above this line is buried into the hydrophobic zone, whereas that below the line is exposed to water. Interestingly, the interface corresponds well to the upper boundary of the polar pattern on the surface: the helix inserts itself into the membrane with its hydrophobic part corresponding to residues Val-9 and Lys-6 (partly). Because of the tilted orientation of helix 6–11 with respect to the membrane plane, other nonpolar areas on the MHP map (assigned to residues Pro-8 and Thr-11) are located away from the interface. These results are not evident from the sequence analysis only because it is difficult to predict that Lys-6 will strongly interact with the membrane.

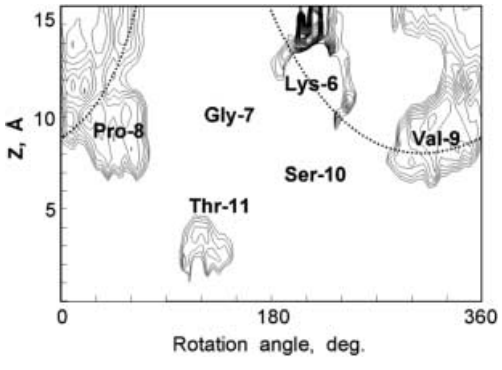

Fig. 6. 2D isopotential maps of the molecular hydrophobicity potential (*MHP*) on the surface of the α-helical peptide 6–11 of $N_{1–15}$–EL. The structure of the peptide corresponds to the lowest-energy state found as the result of the Monte Carlo simulation in membrane-mimetic media. The value on the *x*-axis corresponds to the rotation angle around the helix axis; the parameter on *y*-axis is the distance along the helix axis. The MHP is expressed in arbitrary units (a.u.). Only the hydrophobic areas with MHP > 0.09 a.u. are shown. Contour intervals are 0.015 a.u. The positions of the residues are indicated by *letters* and *numbers*. The *dotted line* shows the boundary of the membrane–water interface

4 Conclusions

In this work we focused our attention on the N-terminal (1–15) part of elafin, the structure of which was not resolved either by X-ray crystallographic or NMR techniques. To explore the conformational preferences of the residues in the region 1–15 of elafin, we performed MC simulations of this peptide in polar (water) and nonpolar (cyclohexane) media, as well as in the heterogeneous three-layer system, which mimics a lipid membrane. Also, a 3.7-ns MD run with explicit water molecules was carried out. The results show that:

1. The apolar environment and the water–lipid interface stabilize the α helix in the region 6–11, while in water it has no regular secondary structure.
2. In the presence of the model membrane the peptide is attached to the bilayer by the amphiphilic α helix 6–11, which inserts itself with its N terminus and forms an angle of about 60° to the membrane plane.

We therefore assume that in nonpolar media the N-terminal part of elafin forms a short helical region, which might act as a membrane anchor.

Acknowledgements. The GROMACS software was licensed to us by the BIOSON Research Institute and the Laboratory of Biophysical Chemistry (Groningen, The Netherlands). We are grateful to W. Braun for providing us with the FANTOM program. E.R.G. is grateful to the University of Reims Champagne-Ardenne for a 2-month professor fellowship. This work was supported by the Ministère de l'Education nationale, de la Recherche et la Technologie, the Russian Foundation for Basic Research (grants 98-04-48823 and 99-07-90464).

References

1. Wiedow O, Schröder J-M, Gregory H, Young JA, Christophers E (1990) J Biol Chem 265: 14791
2. Sallenave J-M, Marsden MD, Ryle AP (1992) Biol Chem Hoppe-Seyler 373: 27
3. Nara K, Ito S, Ito T, Suzuki Y, Ghoneim MA, Tachibana S, Hirose S (1994) J Biochem 115: 441
4. Francart C, Dauchez M, Alix AJP, Lippens G (1997) J Mol Biol 268: 666
5. Tsunemi M, Matsuura Y, Sakakibara S, Katsube Y (1996) Biochemistry 35: 11570
6. Reis PT, Marsden ME, Cunningham GA, Haslett C, Sallenave J-M (1999) FEBS Lett 457: 33
7. Steinert PM, Marekov LN (1995) J Biol Chem 270: 17702
8. Alix AJP, Berjot M, Francart C, Dauchez M, Lippens G (1997) In: Carmona P, et al (eds) Spectroscopy of biological molecules: modern trends. Kluwer, Dordrecht, p 23
9. Deber CM, Li S-C (1995) Biopolymers 37: 295
10. White SH, Wimley WC (1999) Annu Rev Biophys Biomol Struct 28: 319
11. von Freyberg B, Braun W (1991) J Comput Chem 12: 1065
12. Nolde DE, Arseniev AS, Vergoten G, Efremov RG (1997) J Biomol Struct Dyn 15: 1
13. Efremov RG, Nolde DE, Vergoten G, Arseniev AS (1999) Biophys J 76: 2448
14. Volynsky PE, Nolde DE, Arseniev AS, Efremov RG (1999) Internet J Chem v2, article 4, http://www.ijc.com/articles/1999v2/4/
15. Nolde DE, Volynsky PE, Arseniev AS, Efremov RG (2000) Russ J Bioorg Chem 26: 115

16. Némethy G, Pottle MS, Sheraga HA (1983) J Phys Chem 87: 1883
17. Van der Spoel D, van Buuren AR, Apol A, Meulenhoff PJ, Tieleman P, Sijbers ALTM, van Drunen R, Berendsen HJC (1996) GROMACS user manual, version 20. University of Groningen
18. Kabsch W, Sander C (1983) Biopolymers 22: 2577
19. Koradi R, Billeter M, Wüthrich K (1996) J Mol Graphics 14: 51
20. Efremov RG, Gulyaev DI, Vergoten G, Modyanov NN (1992) J Protein Chem 11: 665
21. Efremov RG, Alix AJP (1993) J Biomol Struct Dyn 11: 483
22. Rohl CA, Chakrabartty CL, Baldwin RL (1996) Protein Sci 5: 2623
23. Anonymous ftp site for the program HELIX: cmgm.stanford.edu/pub/helix/helix2
24. Juffer A, Eisenhaber F, Hubbard S, Walther D, Argos P (1995) Protein Sci 4: 2499
25. Blaber M, Zhang X-J, Matthews BW (1993) Science 260: 1637
26. Tieleman DP, Berendsen HJ, Sansom MS (1999) Biophys J 76: 3186
27. Eisenberg D, Weiss RM, Terwilliger TC (1984) Proc Natl Acad Sci USA 81: 140
28. Furet P, Sele A, Cohen NC (1988) J Mol Graphics 6: 182